Electronic Supplementary Material (ESI) for RSC Advances.

Supporting Information for

Probing oxygen reduction and oxygen evolution reactions on bifunctional non-precious metal catalysts for metal-air batteries

Thirupathi Thippani[a], Sudip Mandal, Guanxiong Wang[b], Vijay K. Ramani[b], and R. K. Raman[a,*]

[a]Department of Chemistry,

Indian Institute of Technology Madras, Chennai 600 036 India.

[b]Department of Chemical and Biological Engineering,

Illinois Institute of Technology, Chicago IL 60616, USA

*Author to whom all correspondence should be addressed

E-mail address: rkraman@iitm.ac.in

Table S1 Elemental composition obtained through XPS analysis for the three catalysts

Catalyst	Element (in wt. %)			
	Co	N	O	C
N-MWCNTs-Co-800-20min	0.86	2.2	5.13	91.8
N-MWCNTs-Co-800-60min	1.12	1.85	6.84	90.18
N-MWCNTs-Co-800-120min	0.52	0.92	9.14	89.42

Table S2 Corrosion parameters extracted from the potentiodyanmic Tafel plots

Catalyst	**I_{corr} (µA)**	**E_{corr} (mV vs. Hg/HgO)**	**β_a (mV dec^{-1})**	**β_c (mV dec^{-1})**	**R_p (Ohm cm^2)**
Ketjenblack carbon	21.642	-362	977	23	90
N-MWCNTs-Co-800-120min	2.311	-326	88	43	1048

$$R_p = \frac{1}{i_{corr}(\beta_a + \beta_c)} \frac{\beta_a \beta_c}{2.303}$$

Where,

R_p = polarization resistance

i_{corr} = corrosion current

β_a = anodic tafel constant

β_c = cathodic tafel constant

Fig. S1

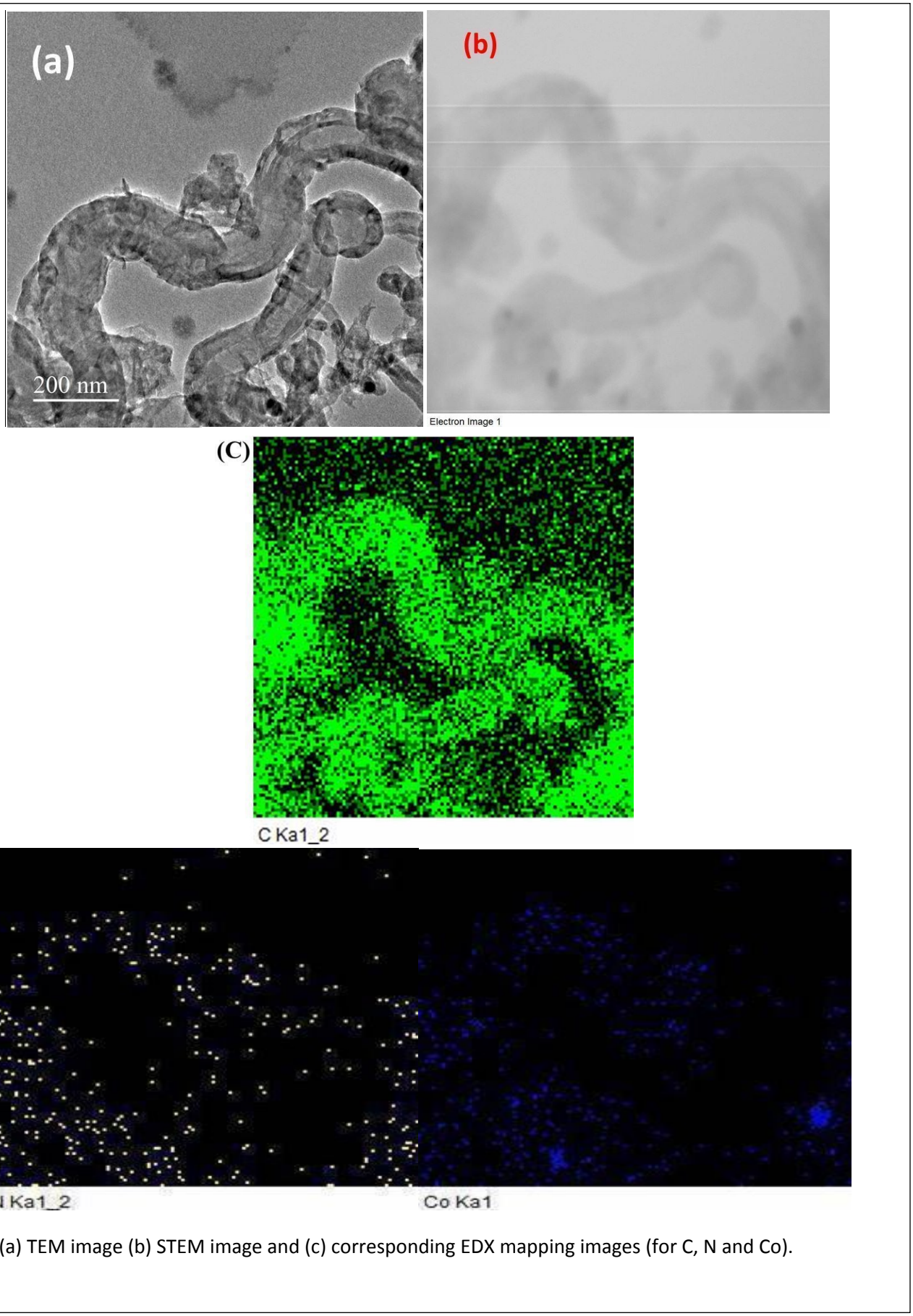

Fig. S1 (a) TEM image (b) STEM image and (c) corresponding EDX mapping images (for C, N and Co).

Fig. S2

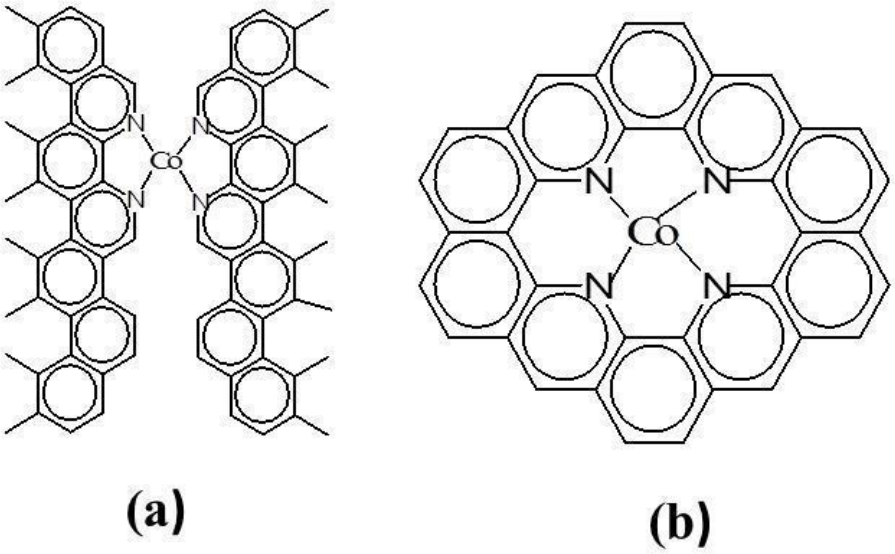

Fig. S2 ORR active site envisioned in the literature (J. P. Dodelet et al. *J. Phys. Chem. B* 2002, *106,* 8705-8713 & Michel Lefèvre *et al. Science* 324, 71 (2009))

Fig. S3

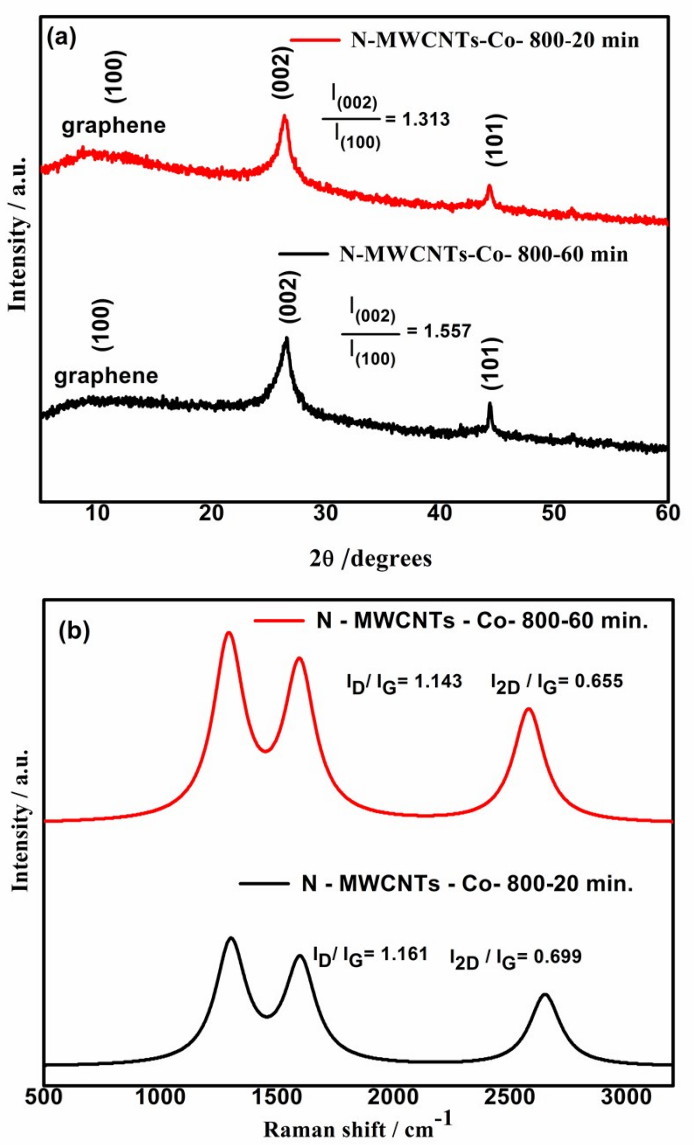

Fig. S3 (a) Powder XRD patterns and (b) Raman spectra of N-MWCNTs-Co-800-20min and N-MWCNTs-Co-800-60min

Fig. S4

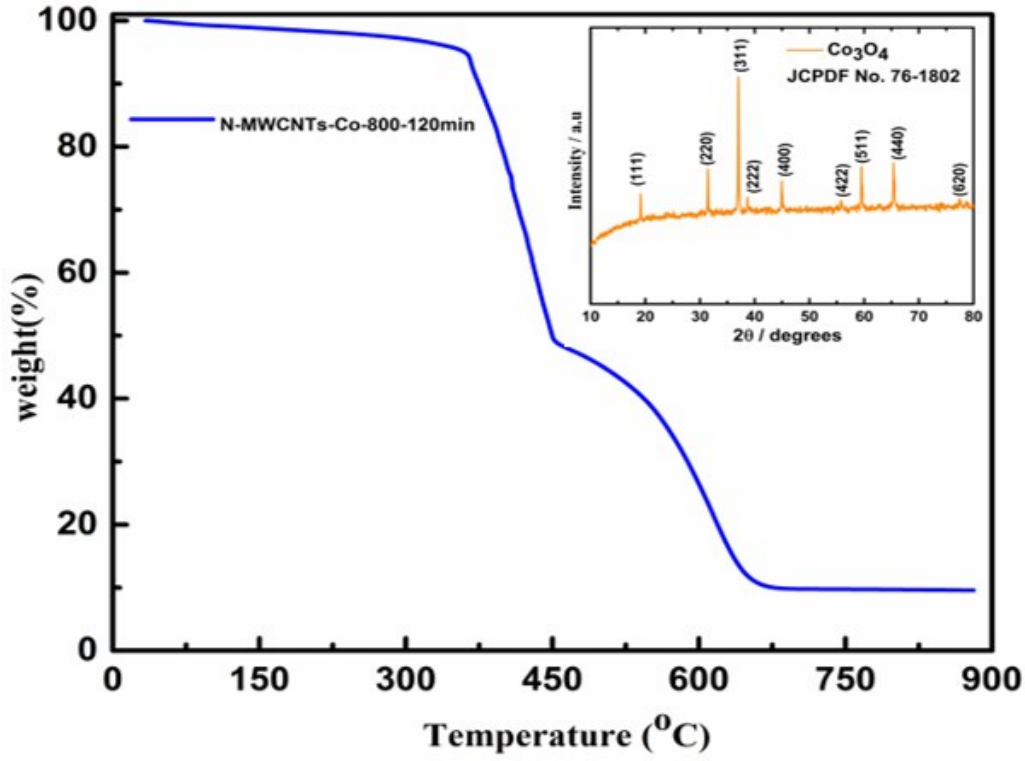

Fig. S4 TGA profile of N-MWCNTs-Co-800-120min and the inset shows the XRD pattern of Co_3O_4.

Fig. S5

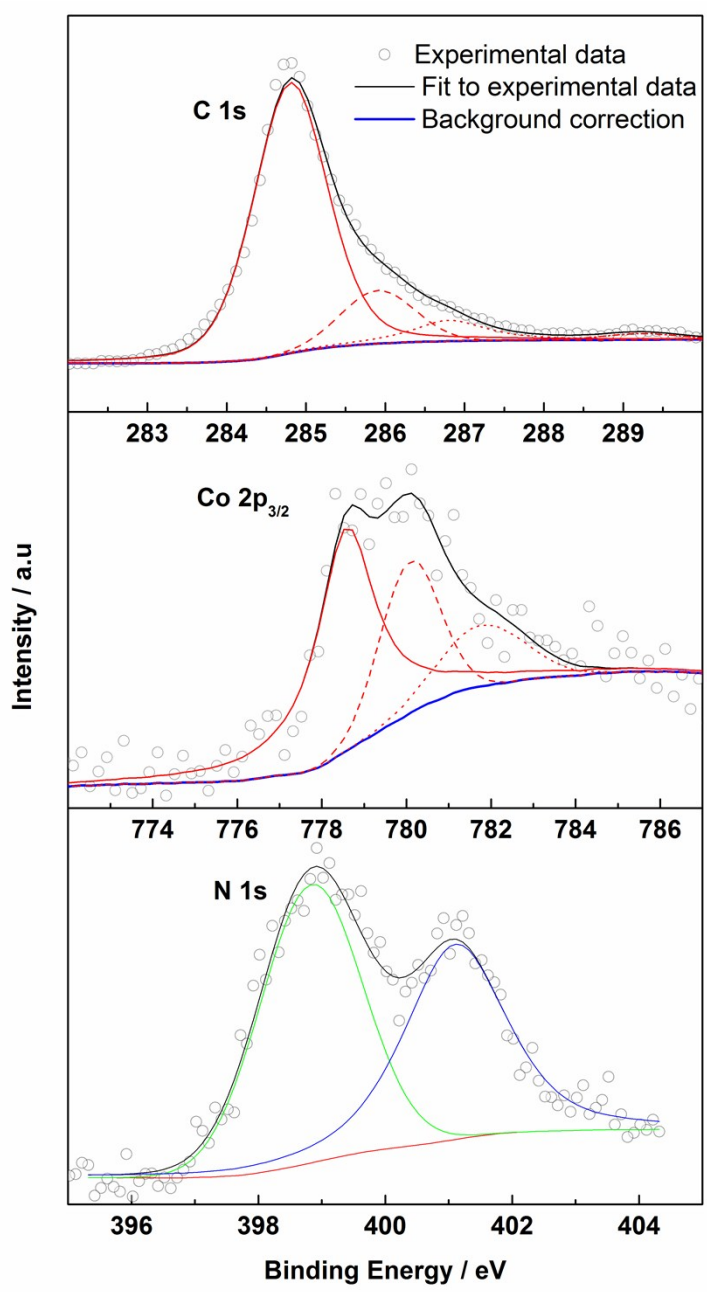

Fig. S5 XPS spectra of N-MWCNTs-Co-800-20min

Fig. S6

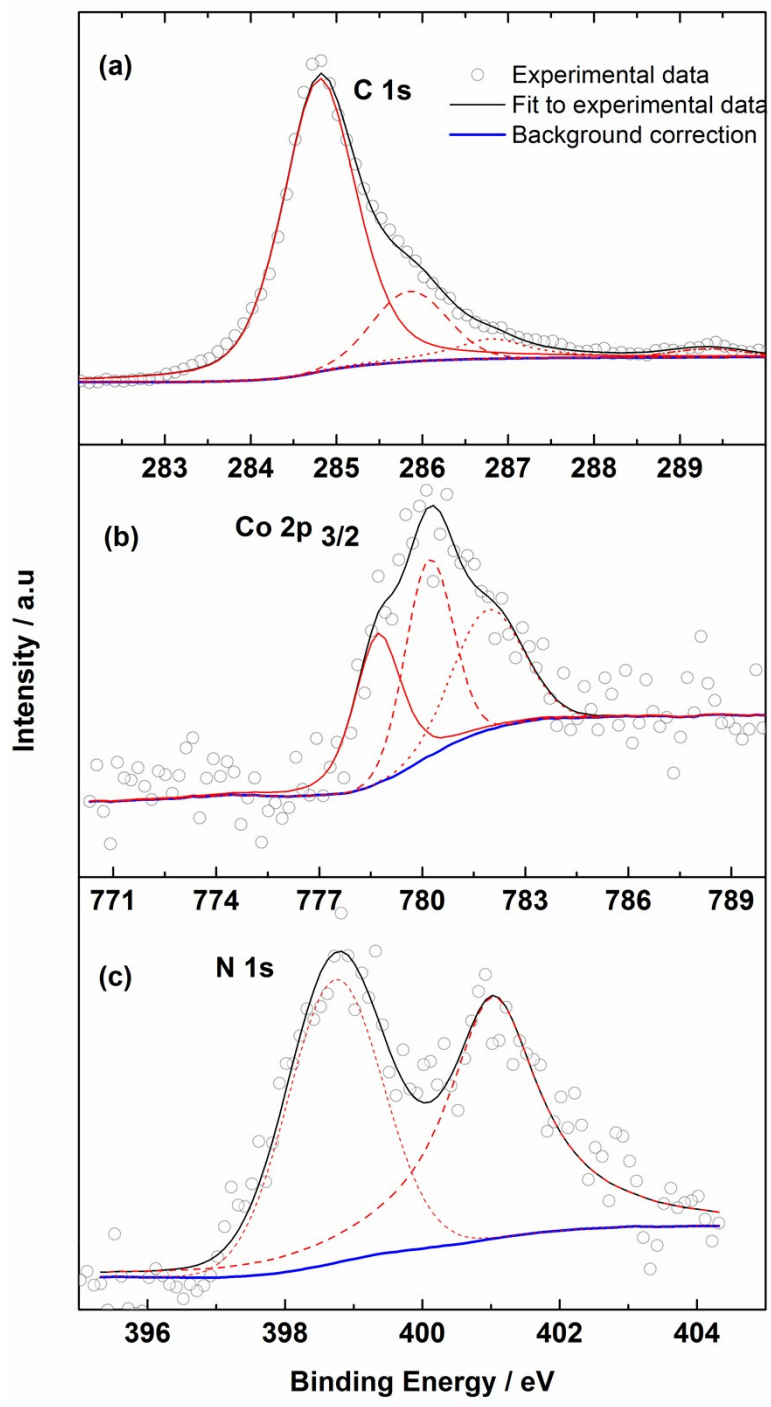

Fig. S6 XPS spectra of N-MWCNTs-Co-800-60min

Fig. S7

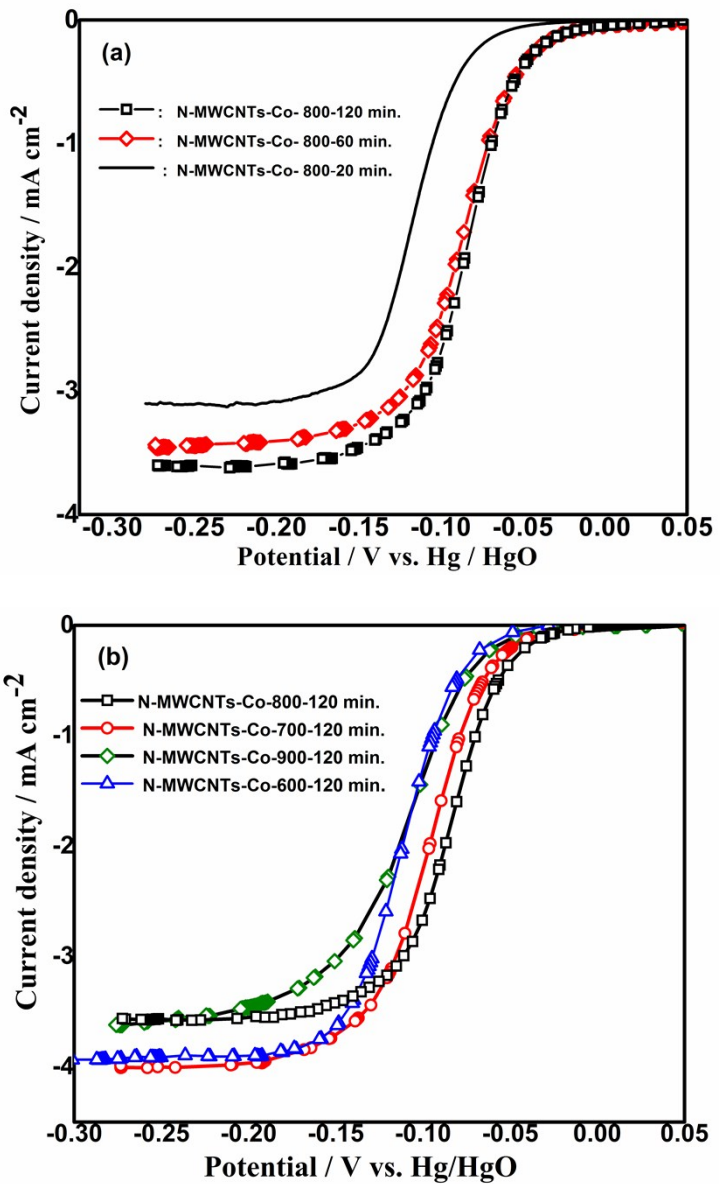

Fig. S7 (a) ORR polarization curves for N-MWCNTs-Co-800-20min, N-MWCNTs-Co800-60min, N-MWCNTs-Co800-120min catalysts and (b) N-MWCNTs-Co-800-120min, N-MWCNTs-Co-700-120min, N-MWCNTs-Co-800-120min and N-MWCNTs-Co-900-120min. Experimental conditions: Oxygen saturated 0.1 M KOH, RDE rotation rate 1600 rpm, catalyst loading 0.2 mg cm^{-2}, scan rate 5 mV s^{-1}.

Fig. S8

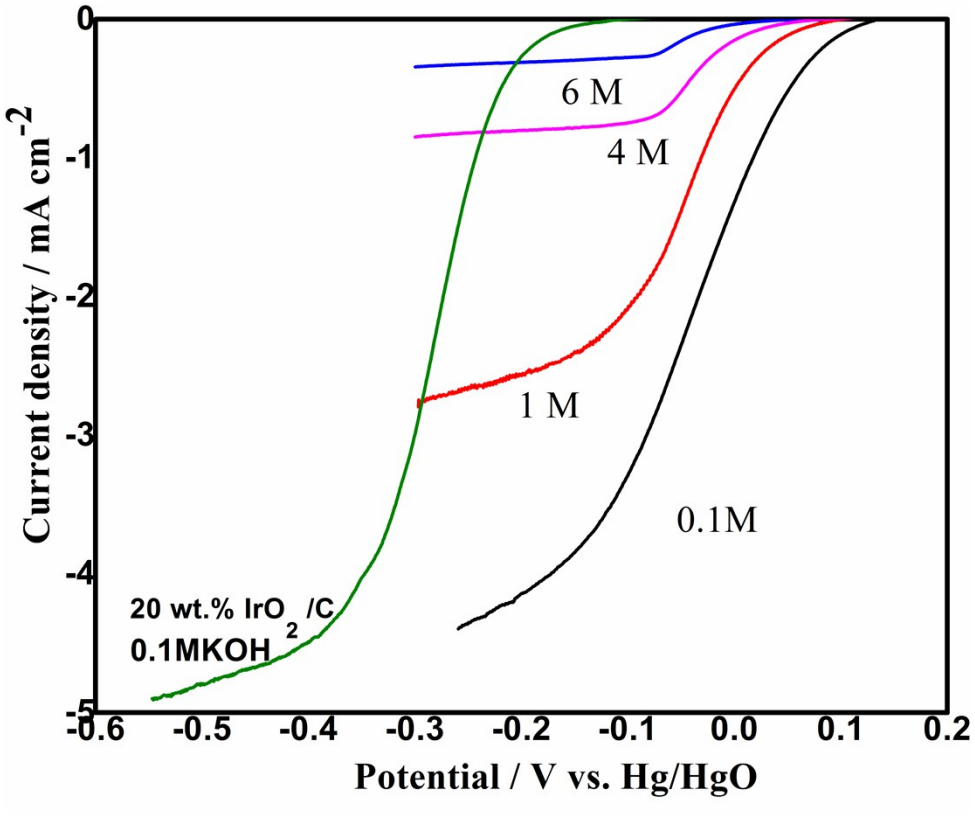

Fig. S8 ORR polarization curves of the 20 wt.% Pt/C measured in O_2-saturated KOH solutions and 20 wt.% IrO_2/C in 0.1 M KOH.

Fig. S9

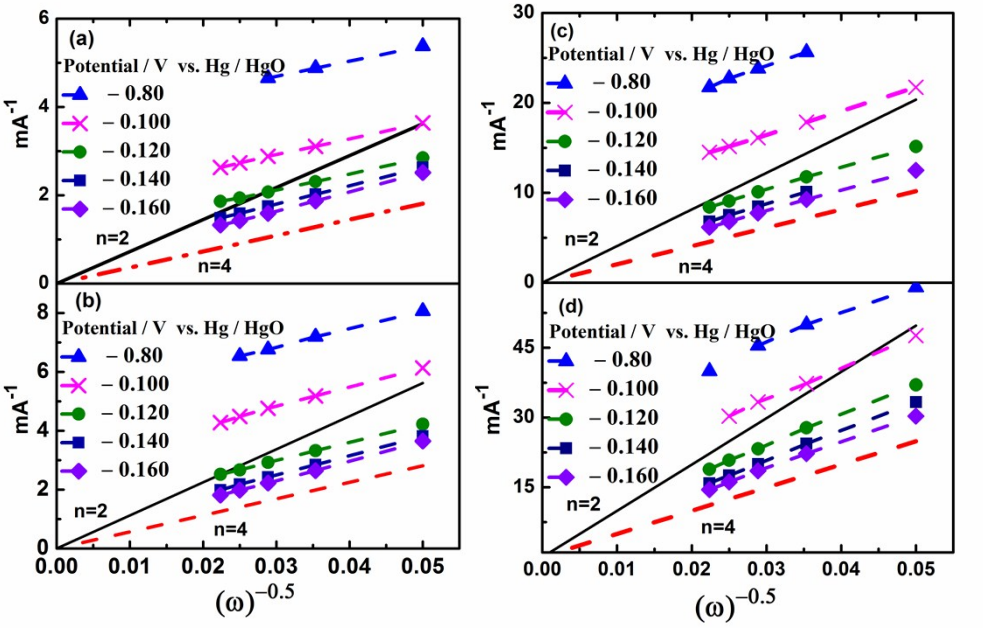

Fig. S9 ORR Koutecky-Levich plots of N-MWCNTs-Co-800-120min in O_2 saturated KOH: (a) 0.1 M (b) 1M (c) 4M and (d) 6M.

As per K-L theory, ORR is assumed to follow first-order kinetics with respect to dissolved oxygen concentration and the measured disk current (i_d) can be expressed as shown below:

$$\frac{1}{i_d} = \frac{1}{i_k} + \frac{1}{i_L} + \frac{1}{i_f} \qquad [1]$$

Where i_k, i_L and i_f are the kinetic current, diffusion-limited current, and diffusion limiting current within the Nafion® ionomer layer respectively.

Furthermore, i_k, i_L and i_f can be expressed by equations 2,3 &4 respectively.

$$i_k = nFAkC_{O_2} \qquad [2]$$

$$i_L = 0.201\, n\, F\, A\, C_{O_2} D_{O_2}^{\frac{2}{3}} v^{\frac{-1}{6}} \omega^{\frac{1}{2}} = B\, n\, \omega^{\frac{1}{2}} \qquad [3]$$

$$i_f = nFAC_{O_2}^f D_{O_2}^f L^{-1} \quad [4]$$

where F is the Faraday constant (96500 C/mole of electrons), A is the geometric area of the disc electrode (0.196 cm^2), C_{O_2}(mol cm^{-3}) is the dissolved oxygen concentration, $D_{O_2}$is the diffusion coefficient of oxygen, υ (cm^2 s^{-1}) is the kinematic viscosity of the electrolyte, $C_{O_2}^f and\ D_{O_2}^f$ are the concentration and diffusion coefficient of O_2 in Nafion® ionomer, ω is the rotation per minute (rpm), k (cm s^{-1}) is the rate constant for ORR and L(cm) is the thickness of Nafion® ionomer layer. In our experiments, the thickness of the Nafion® ionomer layer was calculated to be 0.13 µm, assuming that the density of Nafion® to be 2g cm^{-3}. On assuming that the $C_{O_2}^f and\ D_{O_2}^f$ in Nafion® film is similar to the corresponding values in KOH solution[ref. 47], I_f is calculated to be 606, 398 , 100 and 37 mA cm^{-2} for 0.1M, 1 M 4 M and 6 M KOH solution respectively.

Fig. S10

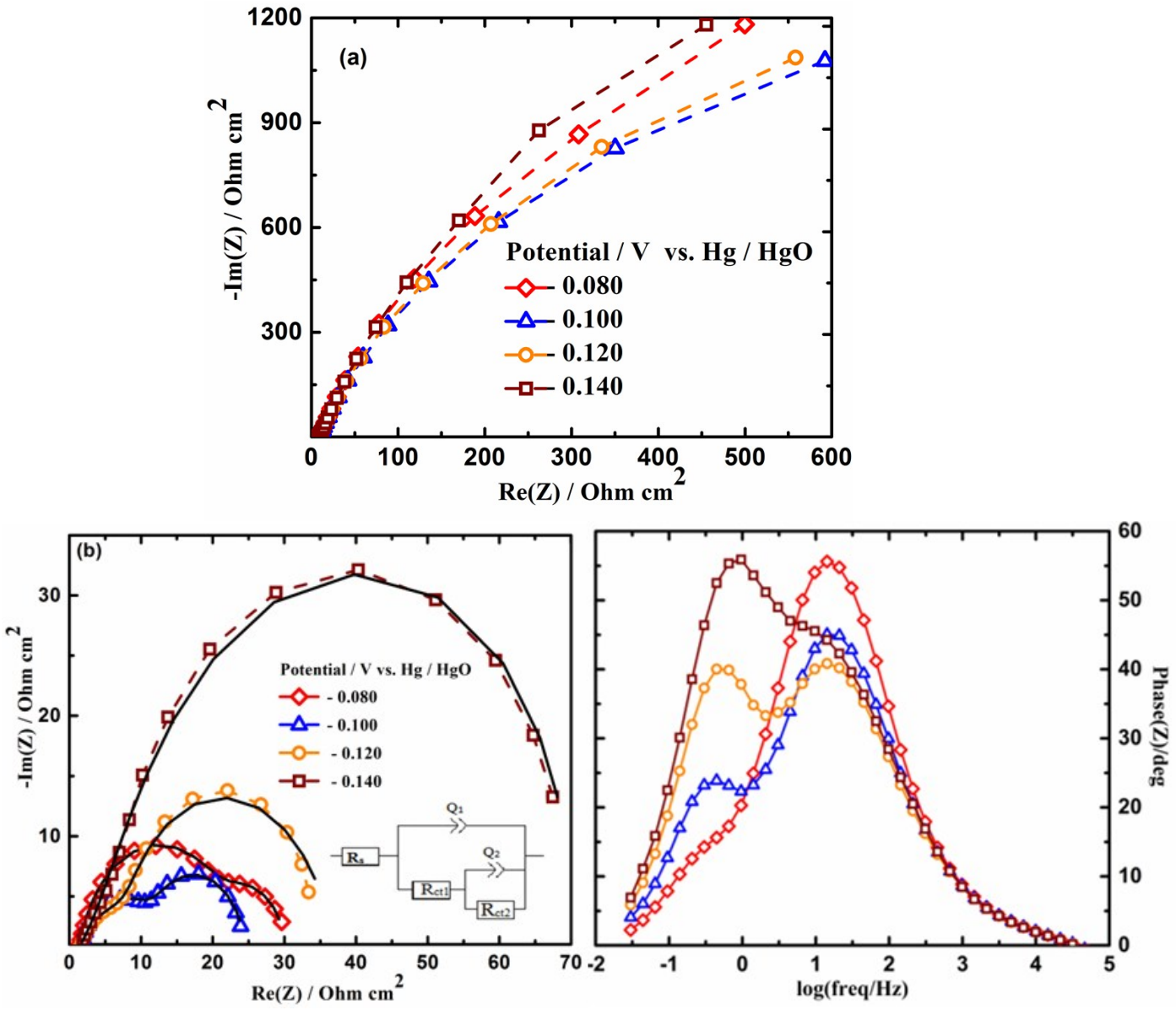
(a)
-Im(Z) / Ohm cm2
Re(Z) / Ohm cm2
Potential / V vs. Hg / HgO
0.080
0.100
0.120
0.140
(b)
-Im(Z) / Ohm cm2
Re(Z) / Ohm cm2
Potential / V vs. Hg / HgO
- 0.080
- 0.100
- 0.120
- 0.140
Rs
Q1
Q2
Rct1
Rct2
Phase(Z)/deg
log(freq/Hz)

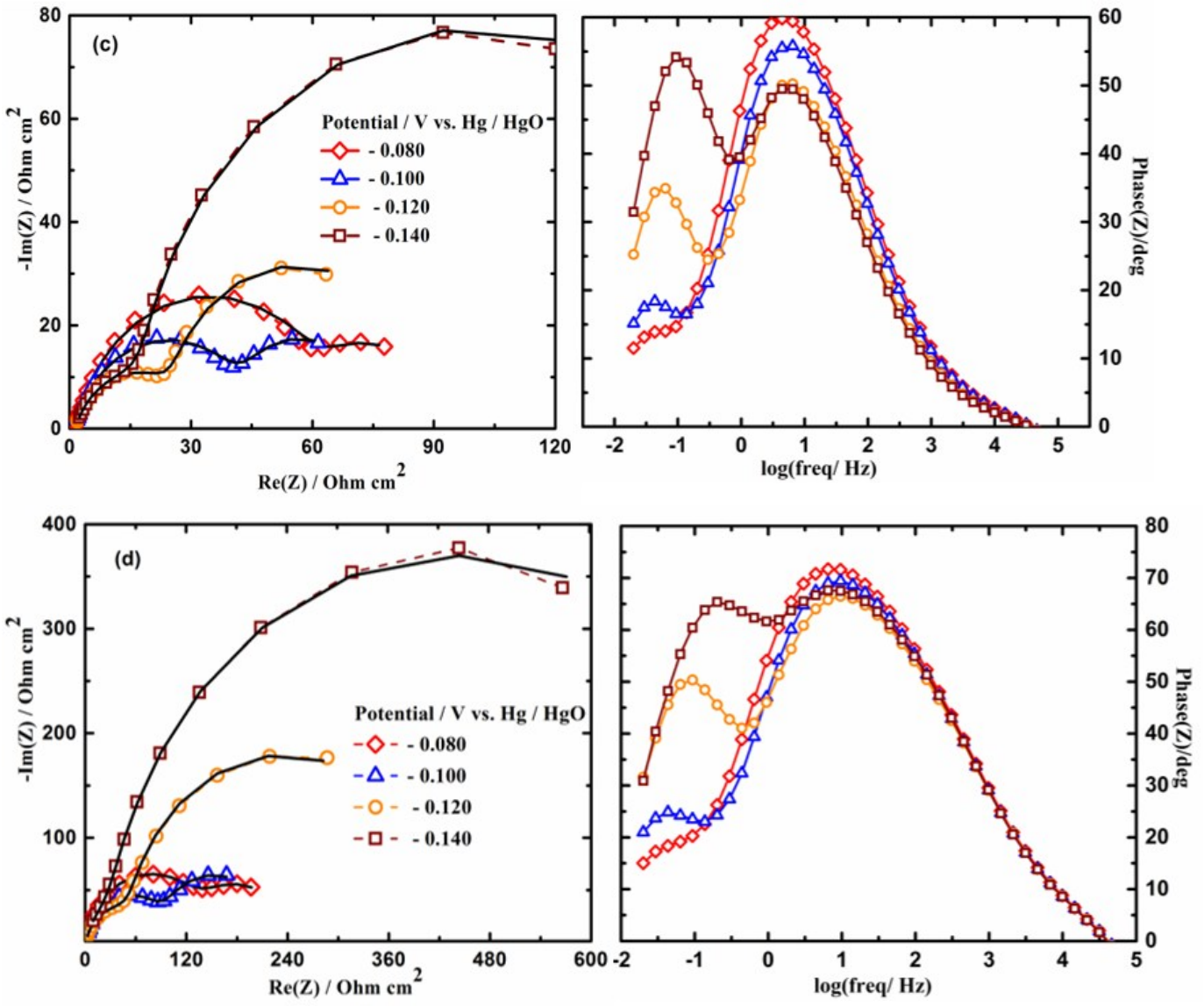

Fig. S10 Nyquist plots obtained using N-MWCNTs-Co-800-120min catalyst coated RDE in (a) N_2-saturated 0.1 M KOH solution and in O_2-saturated (b) 1M (c) 4M and (d) 6M KOH solutions at -0.08, -0.1, -0.12 and -0.14 V vs. Hg/HgO.

Fig. S11

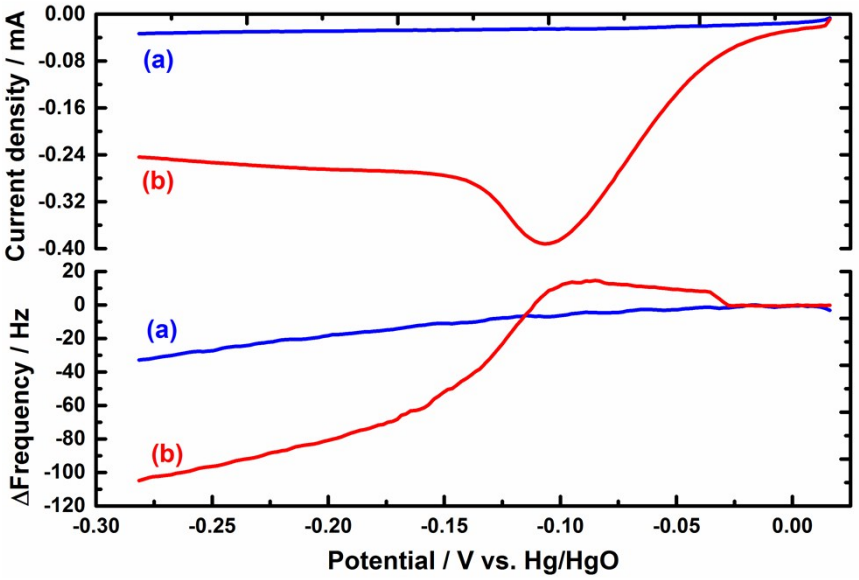

Fig. S11 Linear sweep voltammetry (LSV) of the N-MWCNTs-Co-800^{0}C-120min with EQCM, measured in (a) N_2-saturated and (b) O_2 saturated 0.1 M KOH solution.

Fig. S12

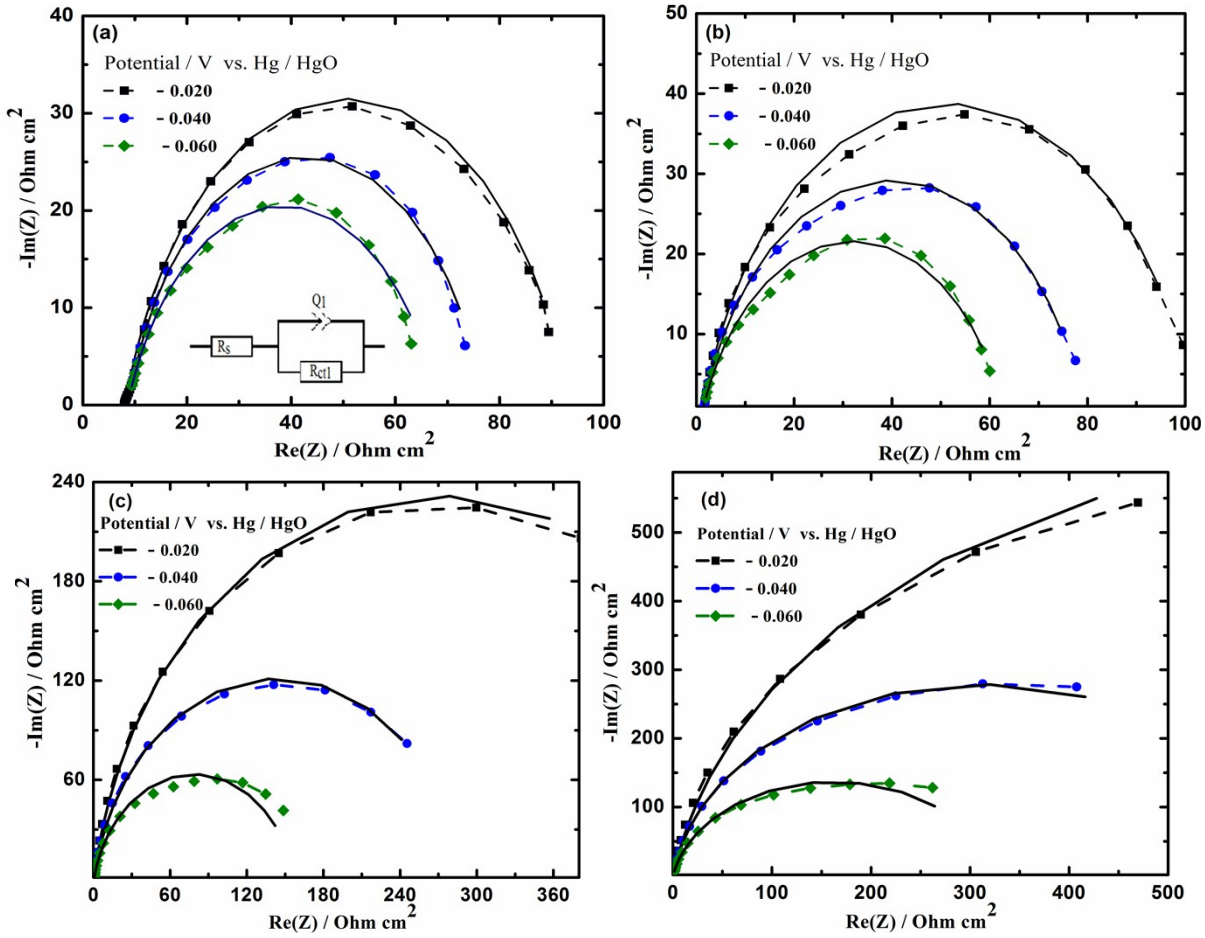

Fig. S12 Nyquist plots obtained using 20 wt.% Pt/C catalyst coated RDE in O_2-saturated (a) 0.1 M,(b) 1 M, (c) 4 M and (d) 6 M KOH solutions at -0.02 , -0.04,and -0.06V vs. Hg/HgO (Circuit used to fit the experimental data is provided as inset in Fig. S12(a)).

Fig. S13

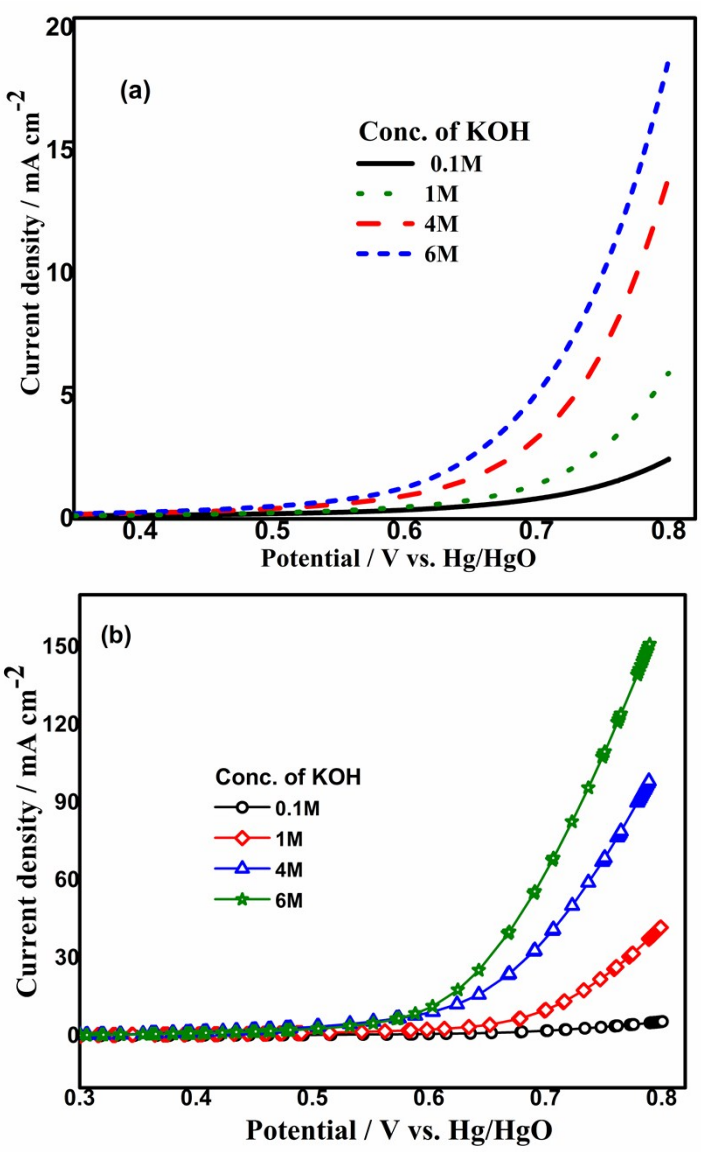

Fig. S13 (a) OER polarization curves of 20 wt.% Pt/C and (b) 20 wt.% IrO_2/C in N_2-saturated 0.1 M, 1 M, 4 M and 6 M KOH solution.

Fig. S14

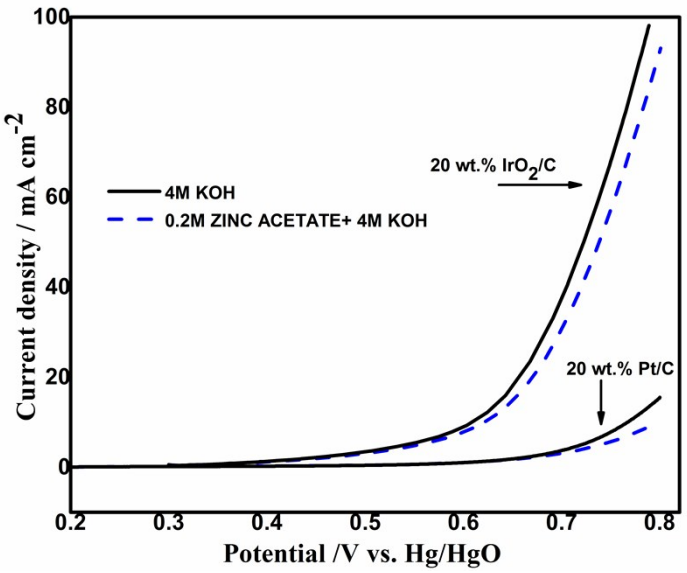

Fig. S14 OER polarization curves of the 20 wt. % Pt/C and 20 wt. % IrO_2/C measured in N_2-saturated 4 M KOH solution with and without 0.2 M zinc acetate.

Fig. S15

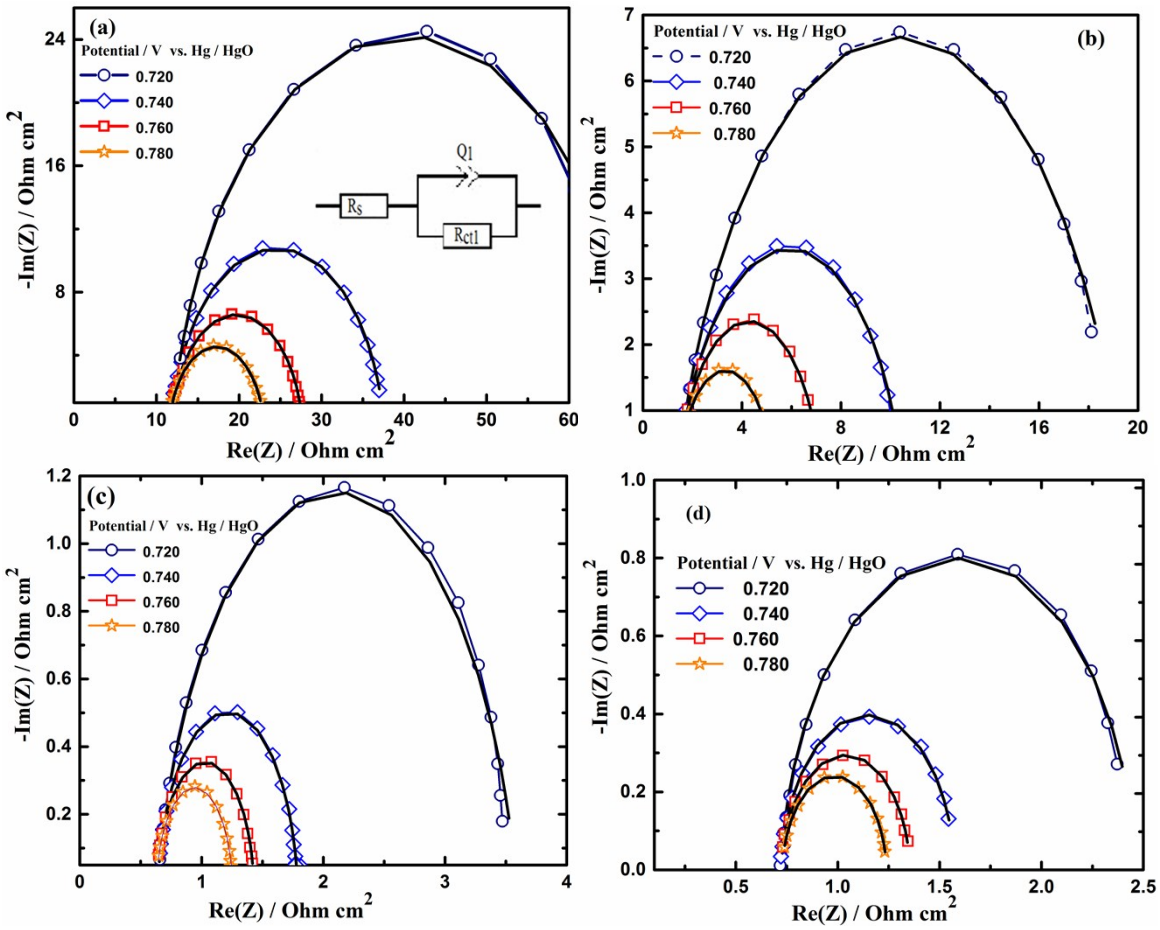

Fig. S15 Nyquist plots obtained using N-MWCNTs-Co-800-120min catalyst coated RDE in N_2-saturated (a) 0.1 M ,(b) 1 M, (c) 4 M and (d) 6 M KOH solutions at 0.720 , 0.740, 0.760 and 0.780V vs. Hg/HgO (Circuit used to fit the experimental data is provided as inset in Fig. S15 (a)).

Fig. S16

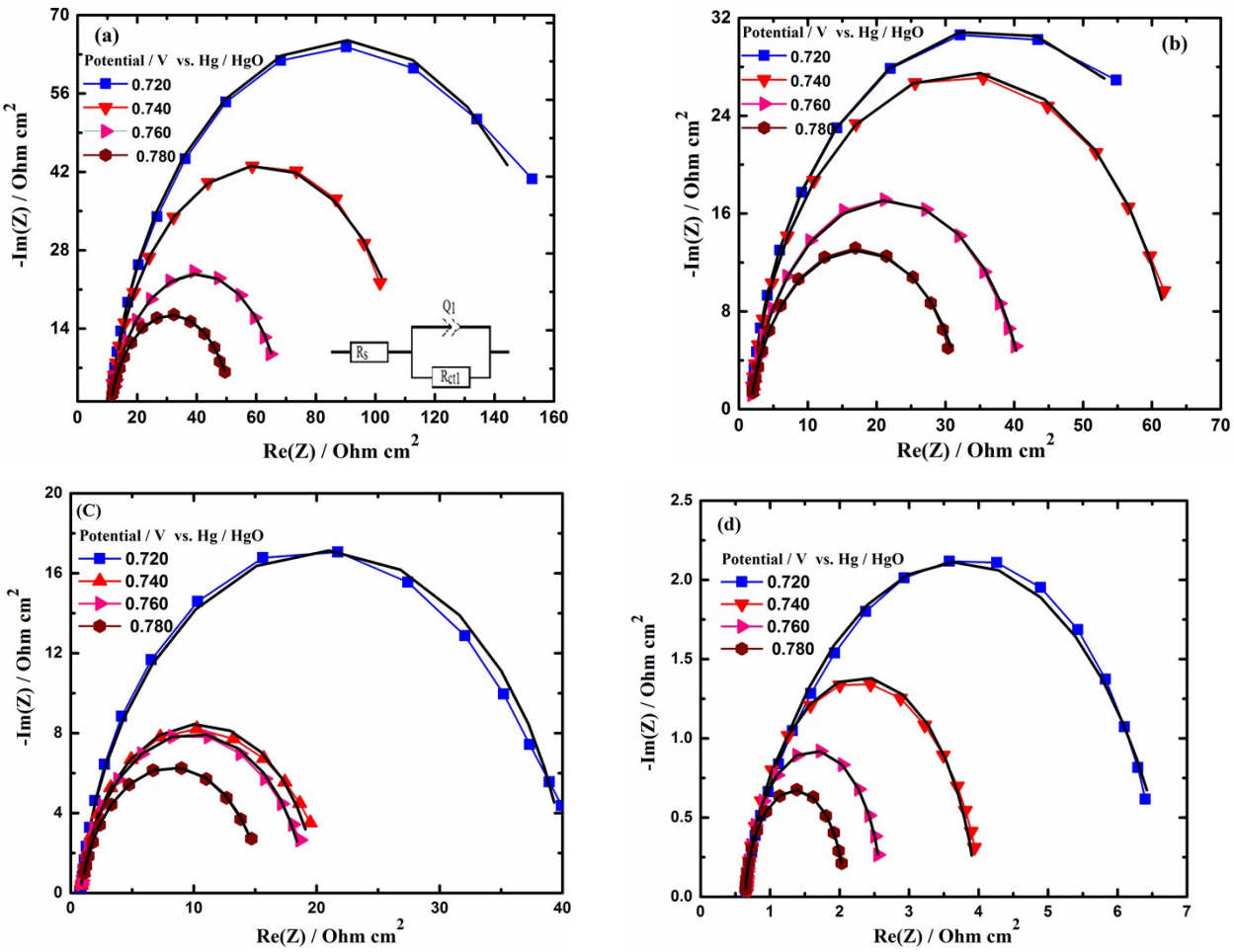

Fig. S16 Nyquist plots obtained using 20 wt.% Pt/C catalyst coated RDE in N_2-saturated (a) 0.1 M ,(b) 1 M, (c) 4 M and (d) 6 M KOH solutions at 0.720 , 0.740,0.760 and 0.780V vs. Hg/HgO (Circuit used to fit the experimental data is provided as inset in Fig. S16(a)).

Fig. S17

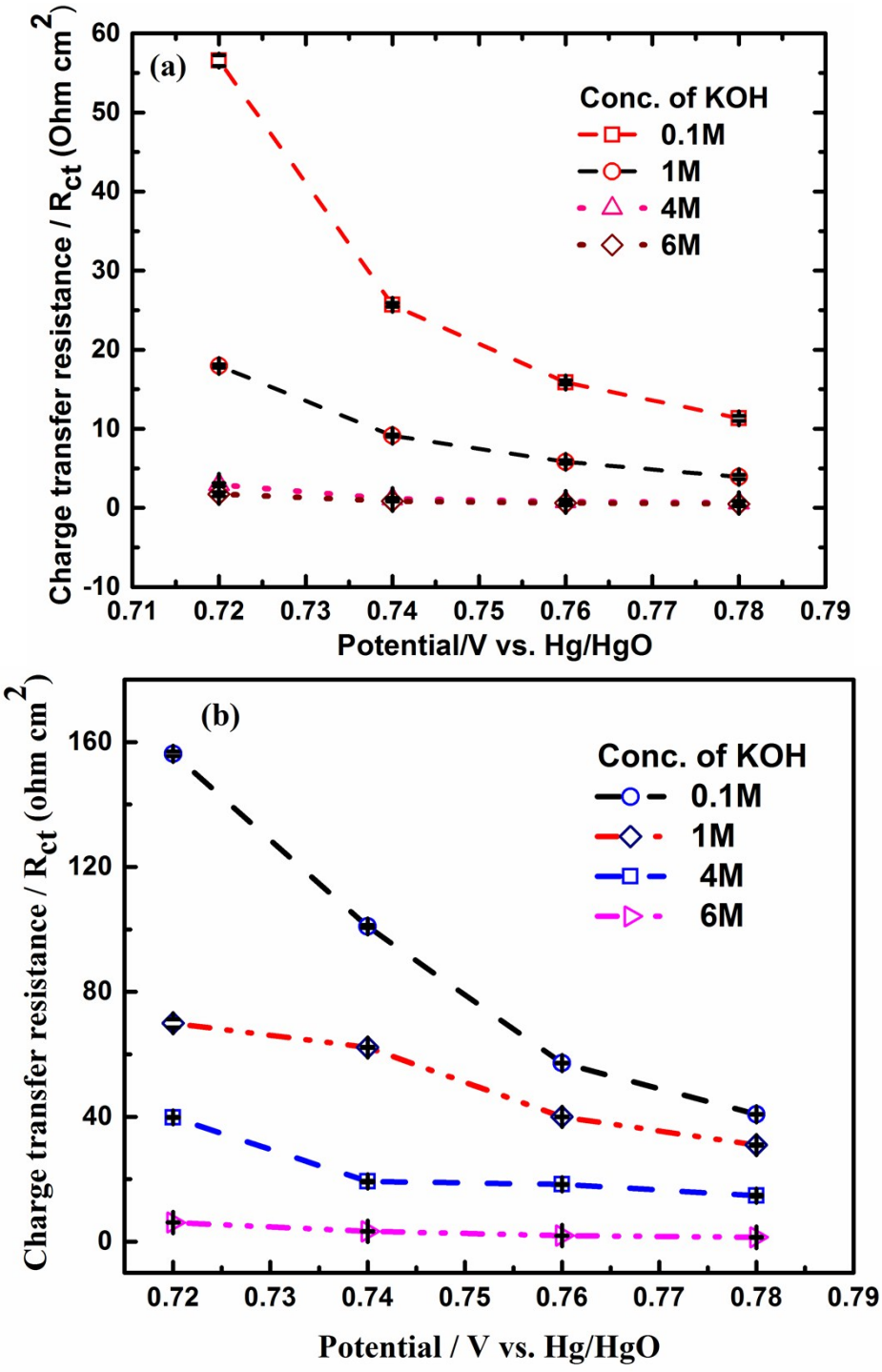

Fig. S17 Plot of R_{ct} versus potential in various KOH solutions for (a) N-MWCNTs-Co-800-120min and (b) 20 wt. % Pt/C catalyst.

Fig. S18

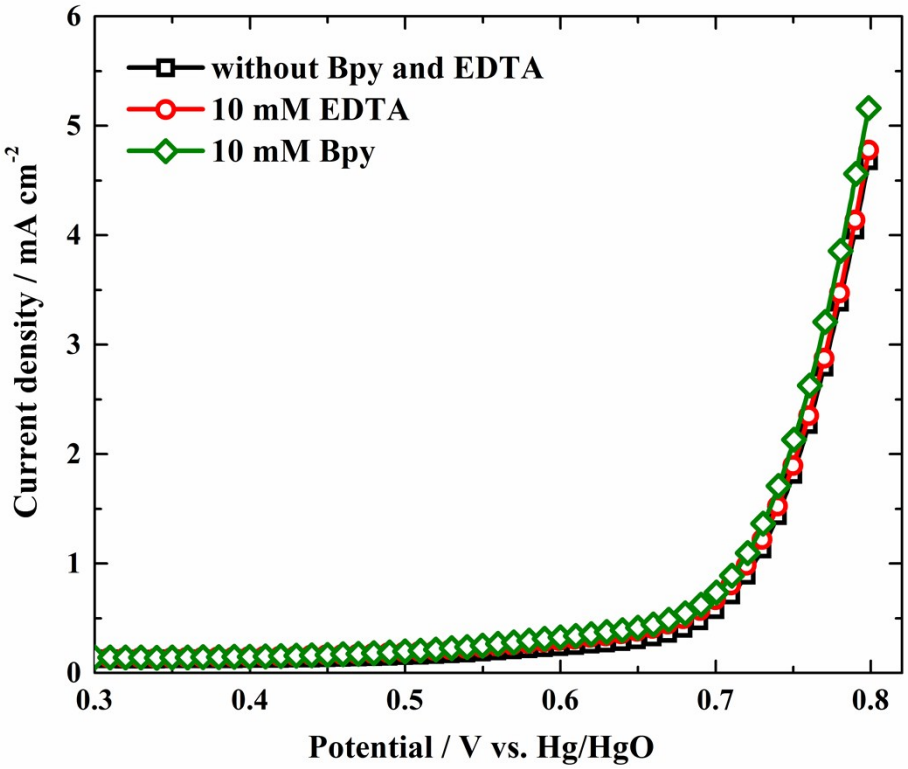

Fig. S18 OER activity of N-MWCNTs-Co-800-120min measured in N_2 saturated 0.1M KOH solutions with and without Bpy and EDTA.

Fig. S19

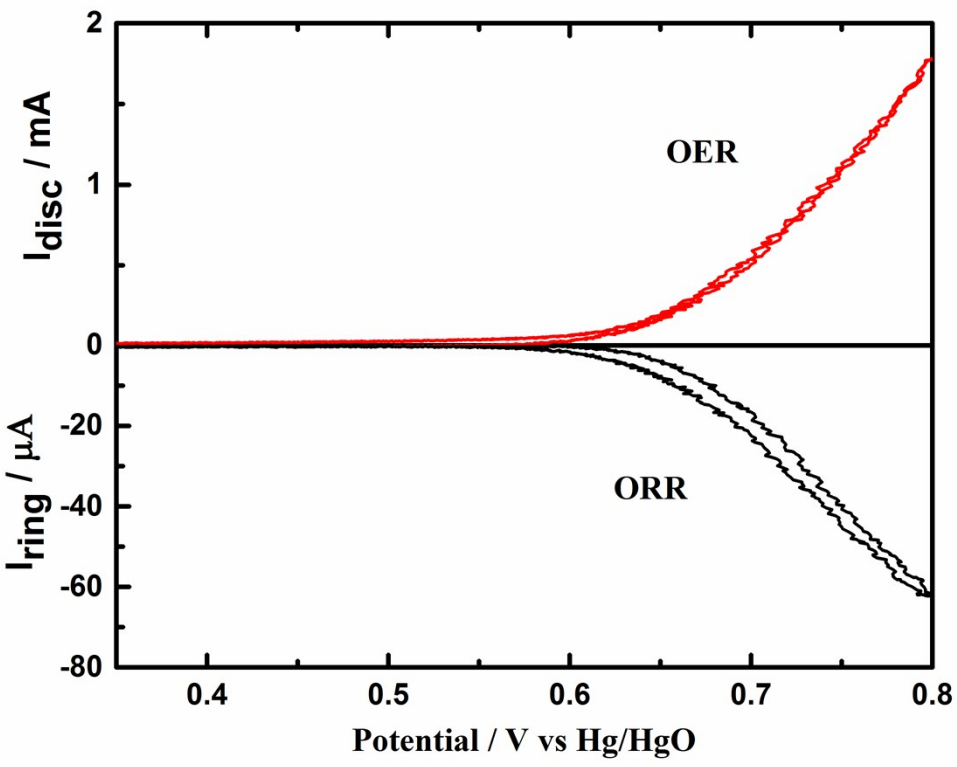

Fig. S19 OER and ORR polarization measured at the disk and ring respectively in 0.1M KOH N_2– saturated solution of N-MWCNTs-Co-800-120 min.

Fig. S20

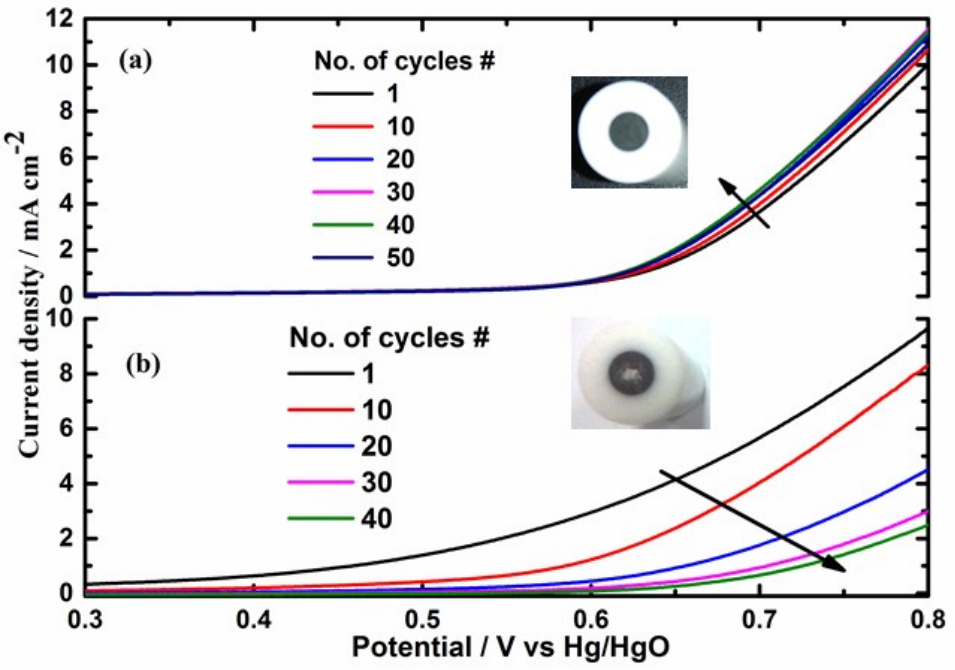

Fig. S20 50 cycles of OER polarization curves of the (a) N- N-MWCNTs-Co-800-120min and (b) Ketjenblack carbon measured in N_2-saturated 0.1 M KOH solution.

Fig. S21

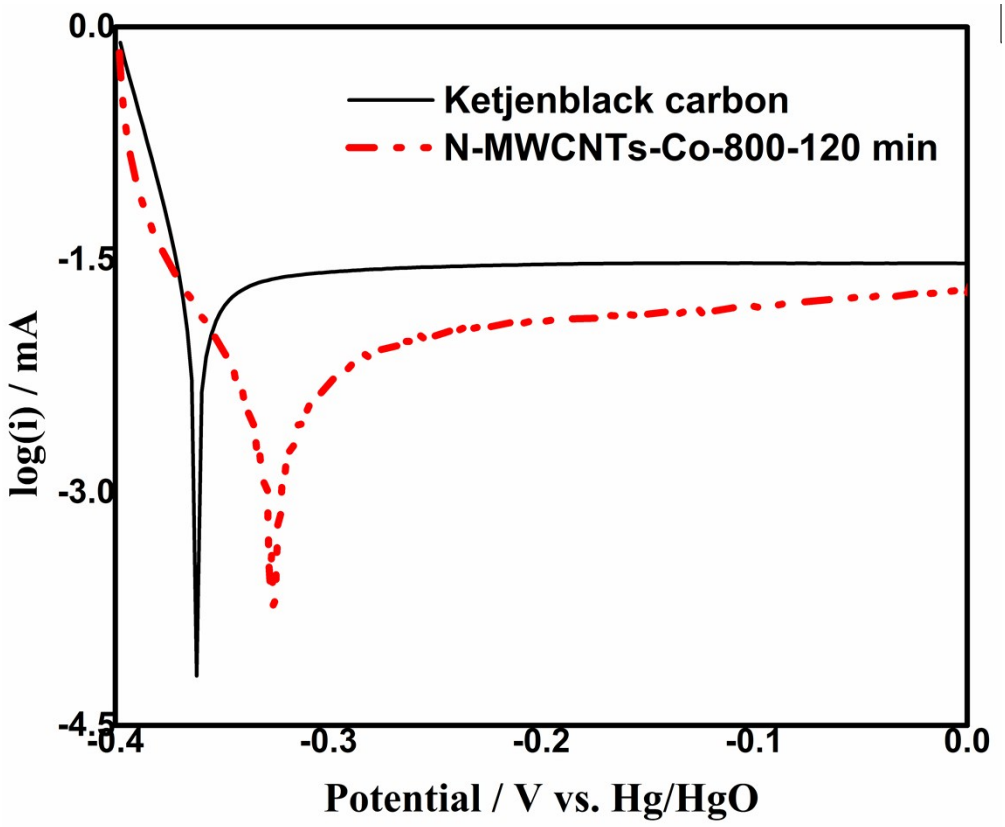

Fig. S21 Potentiodynamic polarization curves for Ketjenblack carbon (reference) and N-MWCNTs-Co-800-120min measured in 0.1 KOH solution at 20 mV s^{-1} scan rate.

Fig. S22

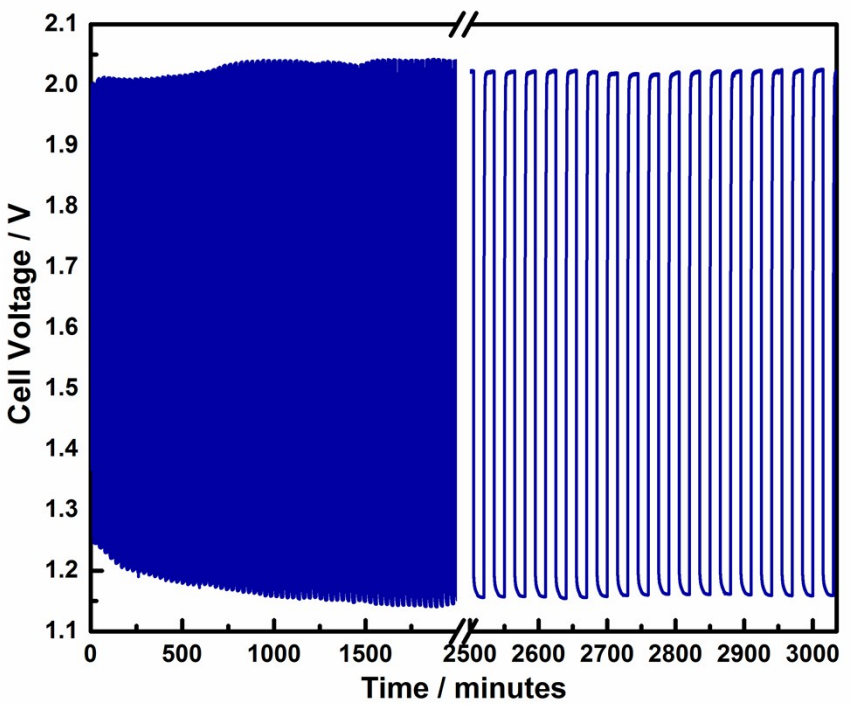

Fig.S22 Charge-discharge curves of a zinc-air battery measured at 0.5 A g^{-1} current density (one cycle includes 15 min of discharge followed by 15 min of charge). Catalyst used is N-MWCNTs-Co-800-120min.

Fig. S23

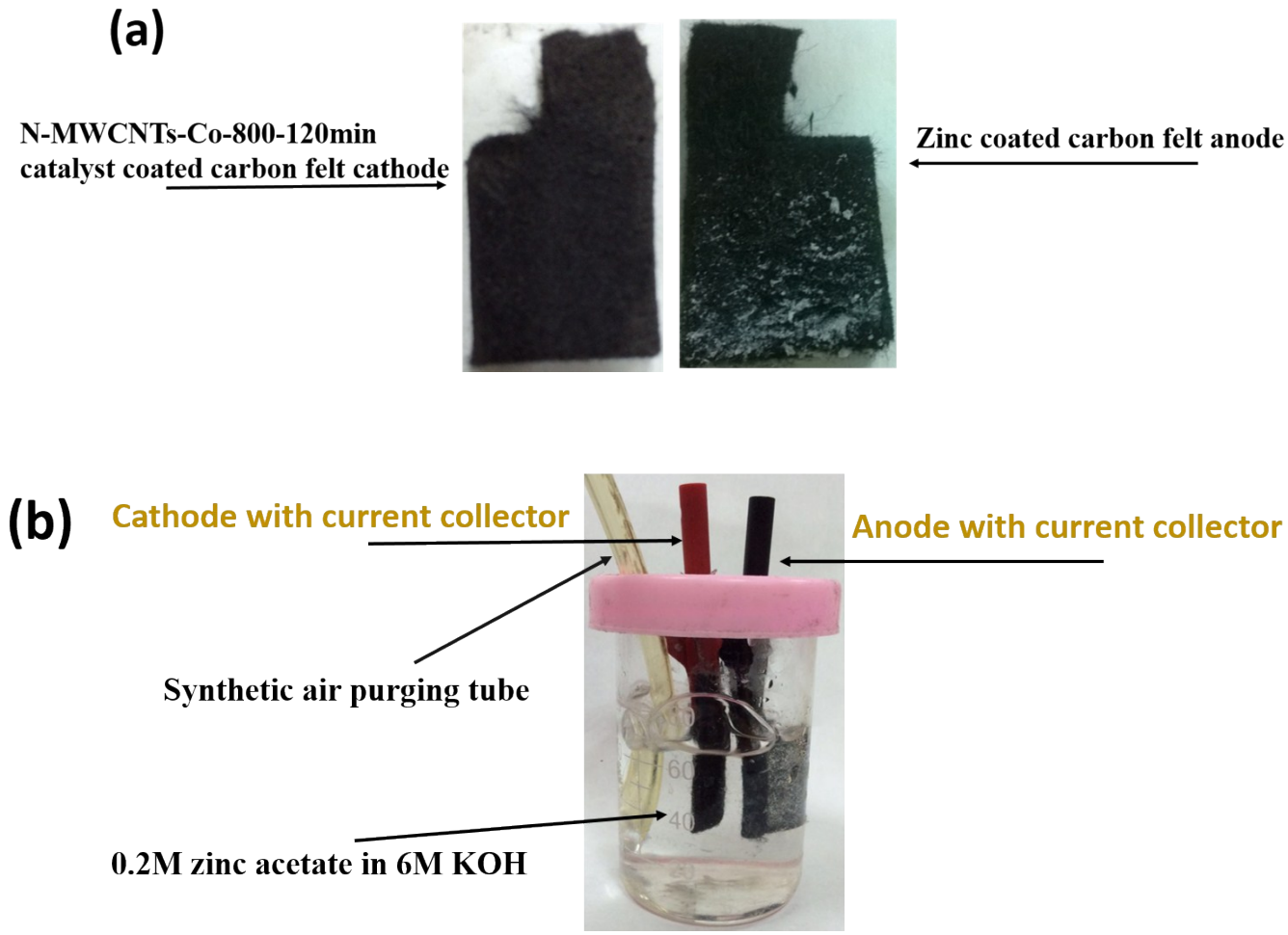

Fig. S23 Shows the (a) photograph of the electrodes N-MWCNTs-Co-800-120min and zinc coated carbon felts respectively and (b) the experimental zinc-air battery setup.

Fig.S24

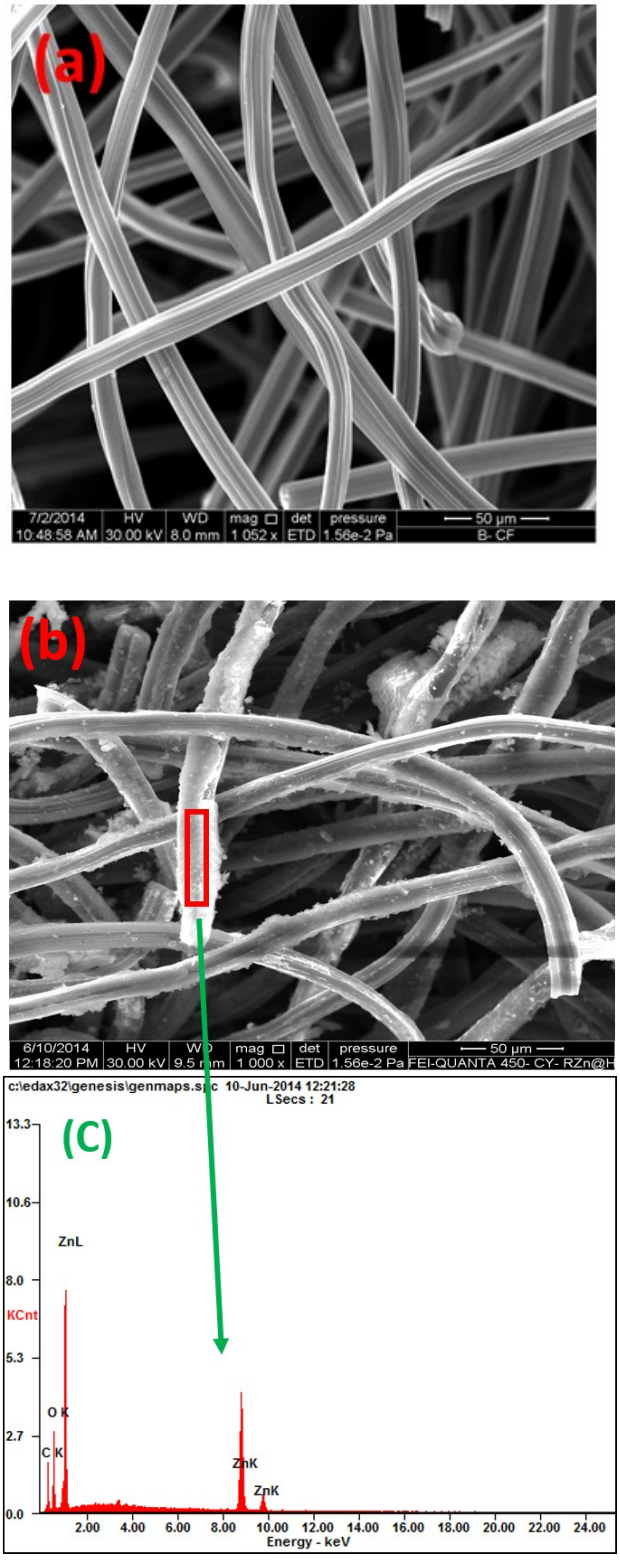

Fig.S24 Compares the SEM micrograph of the (a) carbon felt, (b) zinc-coated carbon felt and (c) EDAX performed on (b).